Solar flare and CME predictions using numerical MHD simulations

Alexander I. Podgorny[1], Igor M. Podgorny[2] and Shigeyuki Minami[3]

[1] *Lebedev Physical Institute, Moscow, 119 991, Russia*
podgorny@fian.fiandns.mipt.ru
[2] *Institute for Astronomy, RAN, Moscow, 109 017, Russia*
[3] *Osaka City University, Sumiyoshi-ku, Osaka 558-8585*

Abstract: According to observational and theoretical data the solar flare radiation and coronal mass ejection (CME) are manifestations of the same explosive process, which takes place high in the solar corona. In some solar flares one of these manifestations can be weak and can not be observed, in other flares both of these manifestations are present. CMEs are the most important cause of substorm appearances in the magnetosphere. For solar flare and CME predictions, it is need to have information about main processes of these explosive phenomena and to estimate the possibility of their occurrences. The energy for solar flare can be accumulated in a current sheet. For MHD simulation of this process the program PERESVET is developed that uses observed distributions of magnetic field on the photosphere as the boundary conditions. The MHD simulation showed, that the current sheet can be vertical, horizontal, or inclined to some angles to the photosphere depending on the magnetic field distribution on the photosphere and its evolution. The vertical current sheet can produce the CME, because the magnetic tension force accelerates plasma from the Sun. The CME prognosis is based on information about the position of current sheet in the solar corona.

key words: flare, CME, MHD, current sheet

1. Introduction

Usually the largest substorms in the Earth's magnetosphere are caused by interplanetary disturbances, which are produced by coronal mass ejections (CMEs) and come from the Sun. The basic physical phenomenon is the same for flares and CMEs, which was confirmed by Zhang *et al.* (2001) for several major events. Earlier the association between flares and CME was discussed by Dryer (1996).

Many data including the X-rays observations of a flare by Yohkoh satellite (Hiei and Hundhausen, 1996) show that initial energy release of such flare process takes place high in the solar corona. The flare energy can be accumulated in a current sheet (CS), which is created in the corona above an active region. MHD simulations have demonstrated that the disturbances, which come from the photosphere, are focused in the vicinity of a singular line of the magnetic field producing the current sheet. Also, a CS can be created by floating up a new magnetic field, which is directed oppositely to

the pre-existing one. The instability of the CS produces the explosive release of the sheet magnetic energy.

According to the flare electrodynamical model (Podgorny and Podgorny, 1992) the energy is transferred from the CS to the lower layers of solar atmosphere by field-aligned currents caused by Hall electric field in the sheet. Coronal mass ejection (CME) appears because of plasma acceleration along the CS by magnetic tension. On the basis of simulation results and observational data it can be concluded that the solar flare and CME are associated. Both of them are the manifestation of the same explosive process.

MHD simulations, which use magnetic charts as boundary conditions, can improve the quality of solar flare and CME prediction.

2. MHD equations and initial conditions

The system of MHD equations for compressive plasma with all dissipative terms is given in dimensionless form:

$$\frac{\partial \mathbf{B}}{\partial t} = \text{rot}(\mathbf{V} \times \mathbf{B}) - \frac{1}{Re_m} \text{rot}\left(\frac{\sigma_0}{\sigma} \text{rot}\mathbf{B}\right), \tag{1}$$

$$\frac{\partial \rho}{\partial t} = -\text{div}(\mathbf{V}\rho), \tag{2}$$

$$\frac{\partial \mathbf{V}}{\partial t} = -(\mathbf{V}, \nabla)\mathbf{V} - \frac{\beta_0}{2\rho} \nabla(\rho T) - \frac{1}{\rho}(\mathbf{B} \times \text{rot}\mathbf{B}) + \frac{1}{Re\rho} \Delta \mathbf{V} + G_g \mathbf{G}, \tag{3}$$

$$\frac{\partial T}{\partial t} = -(\mathbf{V}, \nabla)T - (\gamma-1)T\text{div}\mathbf{V} + (\gamma-1)\frac{2\sigma_0}{Re_m\sigma\beta_0\rho}(\text{rot}\mathbf{B})^2 - (\gamma-1)G_q\rho L'(T)$$
$$+ \frac{\gamma-1}{\rho}\text{div}\left(\mathbf{e}_\parallel \kappa_{dl}(\mathbf{e}_\parallel, \nabla T) + \mathbf{e}_{\perp 1}\kappa_{\perp dl}(\mathbf{e}_{\perp 1}, \nabla T) + \mathbf{e}_{\perp 2}\kappa_{\perp dl}(\mathbf{e}_{\perp 2}, \nabla T)\right). \tag{4}$$

The unit of the length L_0 is taken as the size of calculation region $0 \leq x \leq 1$, $0 \leq y \leq 1$, $0 \leq z \leq 1$. The Y-axis is directed perpendicular to the solar surface, the plane of photosphere is the XZ-plane ($y=0$). The unit of the magnetic field B_0 is taken as a representative field value in the active region of the photosphere. The units of the plasma density ρ_0 and temperature T_0 are taken as their initial values, which are accepted to be constant in space. The units of the plasma velocity is taken to be Alfvenic velocity, and the other units of time, the current density, and the dipole moment are taken correspondingly $V_0 = V_A = B_0/\sqrt{4\pi\rho_0}$, $t_0 = L_0/V_0$, $j_0 = cB_0/(4\pi L_0)$, $M_0 = B_0L_0^3$.

In the eqs. (1)–(4), $Re_m = 4\pi\sigma_0V_0L_0/c^2$ is the magnetic Reynolds number for the conductivity σ_0 at the initial temperature T_0, $\sigma/\sigma_0 = T^{3/2}$, $\beta = 8\pi n_0kT_0/B_0^2$ ($n_0 = \rho_0/m_i$, m_i is the ion mass). $Re = L_0V_0/\eta$ is the Reynolds number, η is the viscosity. $G_q = L(T_0)$ $\rho_0 t_0/T_0$, $L(T_{dimensionsl})$ is the radiation function for the ionization equilibrium of solar corona (Cox and Tucker, 1969). $L'(T) = L(T_0T)/L(T_0)$ is the dimensionless radiation function. $\mathbf{e}_\parallel$, $\mathbf{e}_{\perp 1}$, $\mathbf{e}_{\perp 2}$ are the orthogonal unit vectors, that are parallel and perpendicular to the magnetic field respectively. $\kappa_{dl} = \kappa/(\Pi\kappa_0)$ is the dimensionless thermal conductivity along the magnetic lines, $\Pi = \rho_0L_0V_0/\kappa_0$ is the Peclet number, κ_0 is the thermal conductivity for the temperature T_0, $\kappa/\kappa_0 = T^{5/2}$. $\kappa_{\perp dl} = [(\kappa\kappa_0^{-1}\Pi^{-1})(\kappa_B$

$\kappa_{0B}^{-1}\Pi_B^{-1})]/[(\kappa\kappa_0^{-1}\Pi^{-1})+(\kappa_B\kappa_{0B}^{-1}\Pi_B^{-1})]$ is the dimensionless thermal conductivity perpendicular to the magnetic field, $\Pi_B=\rho_0 L_0 V_0/\kappa_{0B}$ is the Peclet number for the thermoconductivity across the strong magnetic field κ_B (when the cyclotron radius is much smaller than free path length); $\kappa_B/\kappa_{0B}=\rho^2 B^{-2}T^{-1/2}$. $G_g\mathbf{G}$ is the dimensionless gravitational acceleration.

The initial field of spots is approximated by the sum of dipole fields. The dipoles with moments $\mathbf{M}_i=(M_{xi}, M_{yi}, M_{zi})$ are located under the photosphere ($y_i<0$).

The calculations are done using the PERESVET code (Podgorny, 1995). It uses the absolutely implicit finite-difference scheme, and solutions are obtained through iteration method. Multilevel time step decreasing in the regions of strong values gradient takes place. The code is written in FORTRAN language. Now the Visual Digital FORTRAN version 5 is used, but the code can be easily adopted to any other FORTRAN language. The code and its description are presented in http://www.lebedev.ru/pages/wwwhomes/podgorny/N/NUM-MET.HTM.

3.   Simulation of the CS creation in the situation close to real

For studying possibilities of flare energy accumulation in the solar corona and for investigation of the CS properties, the simulations have been done for different magnetic field configurations and for different types of magnetic field changes on the photosphere (Podgorny and Podgorny, 1992, 1998; Podgorny, 1995, Podgorny *et al.,* 2000; Bilenko *et al.,* 2002). Here we briefly present some examples of such calculations. Figure 1 shows the results of simulation for the active region NOAA 6654, which produced a flare on May 30, 1991 (0938 UT). Initially the field of four spots is set, which are approximated by vertical dipoles ($M_x=M_z=0$) situated in plane of symmetry $Z=0.5$ under the photosphere at $y=-0.2$. X coordinate and dipole moments M_y are as follows ($x_1=0.43$, $M_{y1}=-0.0215$), ($x_2=0.4575$, $M_{y2}=0.0213$), ($x_3=0.605$, $M_{y3}=-0.0045$), ($x_4=0.765$, $M_{y4}=0.001$). Figure 1a presents the initial magnetic field in the plane $Z=0.5$, field lines are contained in this plane because all dipoles situated in it. The neutral line position (neutral point) is ($x=0.525$, $y=0.05$).

Excitation of the magnetic disturbances on the photosphere under the neutral line is imposed by changing linearly the photospheric magnetic field at $0<t<1$. This field change is introduced by decrease value of dipoles M_{y1} and M_{y4}. At $t>1$ the photospheric magnetic field is maintained constant with $M_{y1}=-0.0175$ and $M_{y4}=0.0004$. These photospheric disturbances (decreasing of $|M_{y1}|$ and $|M_{y4}|$) produce an increase in the magnetic field under the neutral line. The neutral line is displaced upward and simultaneously the CS is created. At $t=35.6$ the neutral point is displaced to the position ($x=0.484$, $y=0.392$). This effect is seen in Fig. 1b. Here the magnetic field is presented in the plane $z=0.5$ in the extending scale. The magnetic field configuration demonstrates a CS appearance. The typical peculiarity of this CS is similar to the all CSs observed in space and the laboratory. CSs always posses the normal component of magnetic field inside the sheet. **The sheet is not a neutral one.** The force $\mathbf{j}\times\mathbf{B}$ accelerates plasma along the sheet in both directions. The magnetic field asymmetry causes the sheet inclination to the photosphere. For $t=35.6$ the angle of sheet inclination becomes $43.7°$. Plasma accelerated upward in this region can be ejected from the
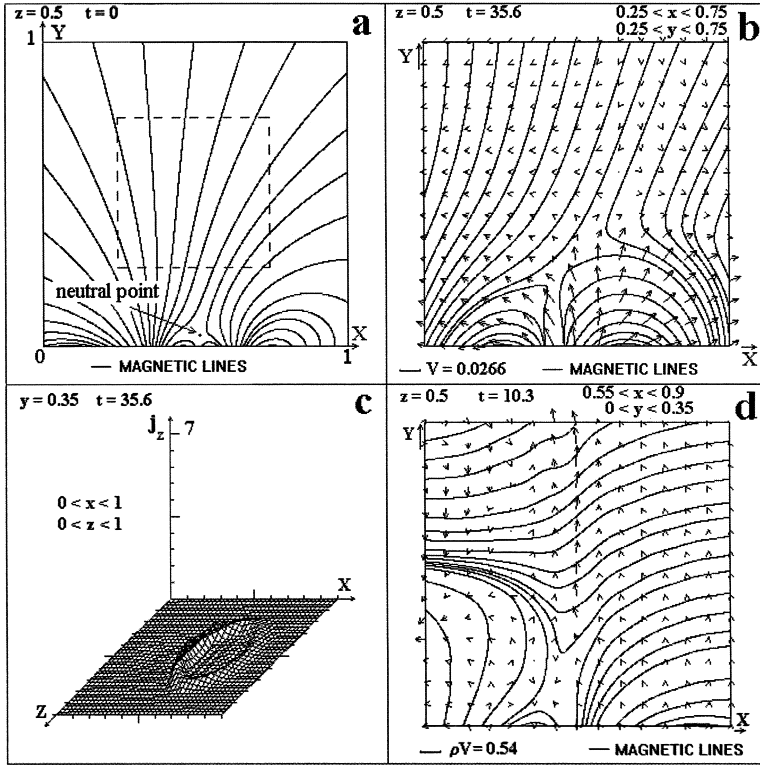
Fig. 1. CS creation in the vicinity of singular line in the solar corona for different types of disturbances: (a), (b), (c)–first and forth dipoles decrease, (d)–first and forth dipoles increase.

corona.

The current distribution of CS in plane $y=0.35$ (Fig. 1c) has the form of oval. The current is distributed around projection of the neutral line top on this plane. The surface of the maximal current density posses the shape of a helmet. It consists in the current sheet itself and a "moustache" of the Petschek type slow shock wave.

Calculations fulfilled by Podgorny and Podgorny (1992, 1998), Podgorny (1995), Podgorny et al. (2000), Bilenko et al. (2002) demonstrate that for different field configurations and different changes in dipole intensities the CS can be inclined at a different angle up to almost $90°$ (vertical sheet). An example of vertical sheet is shown on the Fig. 1d (magnetic lines and velocity vectors). These calculations are done for the initial field of dipoles ($x_1=0.455, y_1=-0.5, M_{y1}=-0.77$), ($x_2=0.4825, y_2=-0.475, M_{y2}=0.79875$), ($x_3=0.675, y_3=-0.475, M_{y3}=-0.16875$), ($x_4=0.79, y_4=-0.5, M_{y4}=0.08$). In these calculations the disturbances are set by increasing of $|M_{y1}|$ and $|M_{y4}|$ at $0<t<1$ up to $M_{y1}=-0.82$ and $M_{y4}=0.1025$. Figure 1d demonstrates the birth of CME, which occurs, because the magnetic tension force in the sheet is directed upward from the Sun. Such effect has been demonstrated by Podgorny and Podgorny (1999).

4. Energy storage for the Bastille flare simulation

Magnetic spot positions of the active region NOAA 9077 before the Bastille flare were extended along a straight line. This line is referred as the line $Y=0$, $Z=0.5$. The most important peculiarity of the magnetic field configuration above this active region can be seen in the plane $Z=0.5$. It permits to trace CS appearance in the vicinity of a neutral line that intersects this plane (Bilenko *et al.,* 2002).

The magnetic field of NOAA 9077 active region is approximated by fields of 7 vertical magnetic dipoles placed below the photosphere. The initial dipole values and positions are presented in dimensional units in Table 1. The dimension of the active region $L_0=260000$ km is taken as the length unit. The average magnetic field above the active region $B_0=300$ Gauss is taken as the magnetic field unit. The dipole magnetic moment unit is $M_0=B_0L_0^3$.

Table 1.   *Dipoles values and positions for CS simulation of Bastille flare.*

N	x	y	z	M_y ($t=0$)	M_y ($t=0.2$)
1	0.14	-0.135	0.5	-0.007	-0.007
2	0.14	-0.135	0.6012	0.005	0.005
3	0.2964	-0.135	0.5	0.01	0.0142
4	0.365	-0.135	0.4888	-0.016	-0.016
5	0.4629	-0.135	0.5	0.0132	0.0132
6	0.6485	-0.135	0.5	-0.013	-0.018
7	0.815	-0.135	0.5	0.0051	0.0051

The numerical investigations are aimed to investigate CS creation in the vicinity of the line. Some preliminary results are reported by Bilenko *et al.* (2002).

Four days prior to the flare the dipole 3 had been increased by factor two. The dipole 6 had been increased between June 10 and 12. Such evolution of the active region is assumed in the numerical experiment presented here.

The magnetic Reynolds number $Re_m=4\pi V_A L\sigma/c^2$ in corona is order of 10^{15}, and frozen-in condition is fulfilled for a very long time. All this time $t_D=Re_m t_A$ the diffusion of magnetic field does not prevent magnetic energy accumulation in the CS. Here $t_A=L/V_A$. The effective (numerical) Re_m in numerical experiment is order of 50. So, for the investigation of CS creation and its evolution in frozen-in condition the time of photospheric disturbance must not considerably exceed t_A. In the numerical experiment shown below t_A is chosen as a unit of time.

In calculation of magnetic energy storage in a CS that appear in the vicinity of singular line due to linear increasing of magnetic field is set during time from $t=0$ to $t=0.2$. The initial and final dipole values are shown in Table 1. After that the photospheric magnetic field is maintained constant. As a result of the imposed changes a magnetic field configuration corresponding to the vertical CS is built. The magnetic field configuration in the CS vicinity is shown in Fig. 2a and 2b. Figure 2a shows lines tangential to projections of **B** vectors on the plane $Z=0.5$ in the extended scale. Such lines can be conventionally considered as "flat magnetic lines". They determine force $\mathbf{j}\times\mathbf{B}/c$ around CS, if the current density vectors are almost perpendicular to the plane.
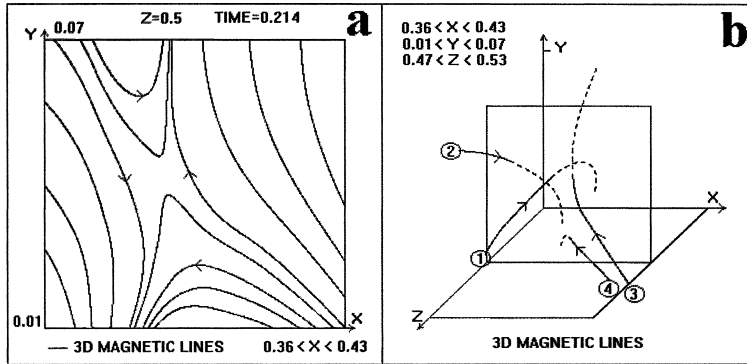
Fig. 2. CS of Bastille flare.

This current component is responsible for the CS creation and energy accumulation.

This CS as all CS in the laboratory and in space possesses a normal magnetic field component. Plasma accelerated upward can be ejected into the interplanetary space producing coronal mass ejection. The most representative lines are presented in Fig. 2b in 3D space. For better perceiving the plane $Z=0.5$ is also presented. Solid lines show segments of magnetic field lines located in front of this plane. Broken lines show segments located behind the plane. Four magnetic lines are shown: 1) Singular line; 2) and 3) Magnetic lines at left and right from the CS; 4) Arch line above the active region. The lines are not contained in the XY plane, because of B_z component existence. Such inclination produces the typical sheared magnetic configuration.

The energy accumulated in the CS magnetic field is the difference between magnetic energy above the active region before the flare and magnetic energy of potential field before the CS creation. In dimensionless units it can be written as $W_{cs}(t) = \int (B^2(t)/2) \, dv - \int (B_{pot}^2(t)/2) dv$. Here, B_{pot} is the potential magnetic field. The result of calculations (Fig. 3) indicates that energy accumulated in the CS before the Bastille event is
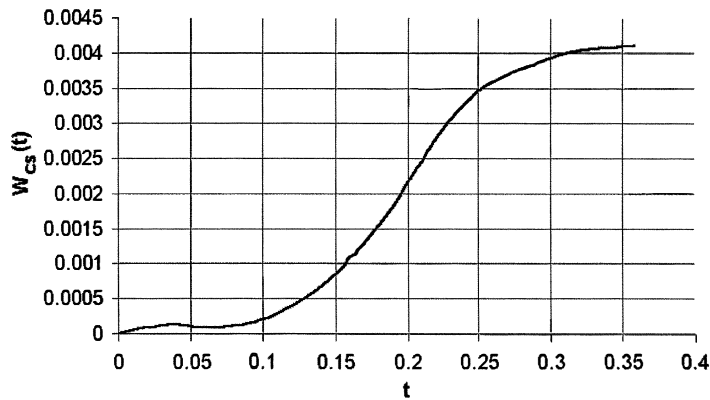

Fig. 3. Energy accumulation in CS.

about 5×10^{32} erg (unit of energy for $B_0=300$ Gauss and $L_0=2.6\times10^{10}$ cm is $(B_0{}^2/4\pi)L_0{}^3$ $=1.26\times10^{35}$ erg).

Plasma outflow along the CS should reduce the CS thickness and initiate instability. As a result the primary flare energy release must occur in corona, and a part of flare energy is transferred to the photosphere.

5.   New magnetic flux emergence

Many indications (Shibata, 1996; Demoulin *et al.,* 1992) show that sometimes the flares occur just after emergence of a new magnetic flux in the active region.   If the old magnetic field does not posses a singular line the temptation arises to explain the flare by interaction of a new magnetic flux with the oppositely directed pre-existing one.   In that case a CS can be produced.   The simplest situation is realized, if two old spots and two new spots are located on the same line, and their fluxes are oppositely directed.   This scenario can be easily observed in a vertical plane that contains the spots.   The main features of such phenomena are revealed in 2D approximation by Podgorny and Podgorny (2001).

At $t=0$ the active region contains two spots approximated by dipoles of opposite polarity: $M_{y1}=0.25$, $x_1=0.1$, $y_1=-0.5$ and $M_{y2}=-0.25$, $x_2=0.45$, $y_2=-0.5$.   After $t=0$ the new two dipoles begin to grow linearly from zero.   Their positions are $x_3=0.78$, $y_3=-0.2$ and $x_4=0.85$, $y_4=-0.2$.   At $t=10$ their magnetic moments become $M_{y3}=0.25$ and $M_{y4}=-0.25$

The magnetic field configuration is dramatically changed by the growth of M_{y3} and M_{y4}.   The plasma moves upward with frozen-in magnetic flux.   The disturbances produced by the upflowing flux propagate with Alfvenic velocity.   Velocity vectors are perpendicular to the magnetic lines, which is typical for MHD disturbances. Simultaneously, a CS is created between the new and old magnetic fluxes.   The high plasma conductivity ($Re_m\gg1$) does not permit to produce the fast reconnection, and the magnetic field energy is accumulated due to CS creation.   The magnetic field lines for $t=5$ are presented in Fig. 4a.   The plasma and magnetic field behavior is seen in Fig. 4b
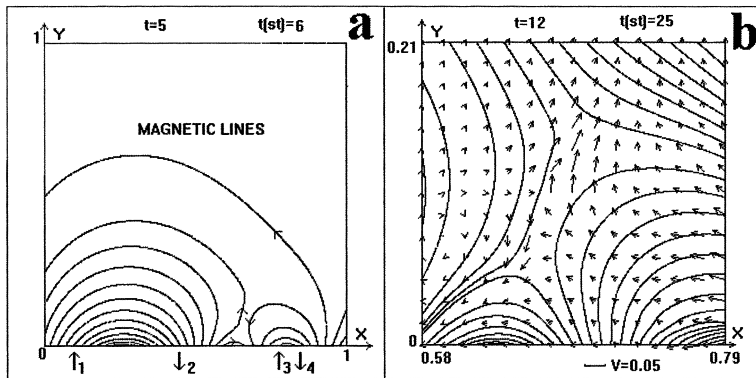

Fig. 4.   CS creation by the floating up the new magnetic field.

in extended scale, where velocity vectors are shown. Plasma flows in the sheet mostly through the right border and is accelerated upward by magnetic tension. Apparently, the plasma flow along the sheet stabilizes the CS. The acceleration downward is not so effective, because of plasma deceleration by the strong magnetic field at the photosphere.

These data demonstrate that the CS, that is created by flowing-up of the new magnetic flux, is practically the same as the sheet obtained by focusing small disturbance in the vicinity of a neutral line.

6.   The possibility of using the MHD simulation for improving solar flare and CME predictions

The mechanism of the solar flare presented above and the results of MHD simulation open a possibility for improving solar flare prediction. It is proposed to add the precursor based on MHD simulations in the solar corona to a typical system of observed precursors, which are used for prognosis. The proposed precursor is based on the assumption that the flare is possible, if a CS is created that accumulates magnetic energy for the flare. Obtained by calculations from observed parameters distributions inside and near the CS, its location in space, the form and angle of sheet inclination to the photosphere also can give some additional precursors for prognosis of flare and CME appearance and their power. If the current sheet position is almost vertical, then an explosive process can produce a CME. In such a case the magnetic tension force accelerates plasma upward from the Sun. It is important to know the angle of sheet inclination to the photosphere, which also can be obtained from the numerical simulation.

The MHD simulations for the situation close to real one have revealed some problems in setting of initial-boundary conditions and solving MHD equations (to obtain a stable solution of the finite-difference scheme). To solve these problems several methods have been developed. Some of them were already realized in the PERESVET code and used in simulations (Podgorny, 1995; Bilenko *et al.,* 2002). The realization of other ones is under way.

6.1.   *The initial-boundary conditions and methods of solution that were used in obtaining the results shown in Figs. 1–4*

The magnetic field distributions in active regions obtained by observations should be used as boundary conditions of the MHD equations. The simplest way of setting the initial conditions is the approximation of spot fields by the fields of vertical dipoles situated under the photosphere on the depth of the order of distances between spots. This field contains the main singularities of a real magnetic field. The method of field approximation by vertical dipoles is already developed and used for results presented here (see also Podgorny and Podgorny, 1992, 1998; Podgorny, 1989, 1995; Podgorny *et al.,* 2000).

To find the other values on the boundary it is necessary to use the fact that for the hyperbolic equations all values on a boundary could not be set independently. There are relationships between them, which are determined by conditions inside the region near the boundary. The solution of the equations on outgoing characteristics under

assumption that dissipative terms can be neglected is used for setting the plasma density ρ and the plasma velocity **V** on a photospheric boundary and for setting free-exit conditions on the nonphotospheric boundary. For this purpose a special procedure is used in the PERESVET code. By solving equations on characteristics the invariants $I(\mathbf{B}, \rho, \mathbf{V})$ are found. The relationships between values **B**, ρ, **V**, the number of which is equal to number of outgoing characteristics are obtained. Using these relationships and values, that are set on the boundary (**B** for the photosphere), the other values (ρ and components of **V**) can be found. For setting free-exit conditions on the non-photospheric boundary it is necessary to have the number of relationships which are equal to the number of values. So, besides the invariants on outgoing characteristics it is necessary to know invariants on the characteristics, which are directed into the region. These invariants have been found from conditions of time independence or zero derivative normal to the boundary ($\partial I/\partial n = 0$).

The calculations show that application of the characteristic method is restricted, so it has been used on initial phase of some calculations to obtain results shown in Figs. 1–4. If the change of values on the space step near the boundary is sufficiently large, then the numerical instability does not permit to solve equations of the characteristics. In this case the values, which are defined on the photospheric boundary by conditions inside the region, and the values on free-exit boundary are found using the following method. The time-independent conditions for the plasma density ρ setting on the boundary is used. The zero first derivative normal to the boundary ($\partial \rho/\partial n = 0$), or zero second derivative normal to the boundary ($\partial \rho^2/\partial n^2 = 0$) can be also used. The last one means extrapolation from two points of numerical net near the boundary. The same conditions are used for the temperature T. It should be noted that these conditions for T are also used in situation suitable for application of the characteristics method for **B**, ρ, **V**, because the term of thermoconductivity is not neglected, and so, the equation for the temperature is not hyperbolic one. For the velocity **V** conditions $\partial \mathbf{V}/\partial n = 0$ and $\partial \mathbf{V}^2/\partial n^2 = 0$ are used. The component **B** normal to the boundary $B_\perp$ is found from div**B** $= 0$. For setting **B** components parallel to the boundary $B_\parallel$ the current component parallel to the boundary $j_\parallel$ is taken to be zero or $\partial j_\parallel/\partial n = 0$. All procedures of setting the values on the boundary are included in the PERESVET code. The condition $\partial j_\parallel/\partial n = 0$ for $B_\parallel$ on the nonphotospheric boundary is used in simulations represented in Fig. 1. Calculations show that these conditions can be applied practically in all situations in the solar corona. It is planned to use these conditions in the majority simulations for solar flare prognosis. In the suitable situation it is planned to use method of characteristics.

The calculations show that the strongest instabilities, which prevented us to obtain correct numerical solution, take place not in the vicinity of singular line, but near the photospheric boundary, where the field gradients are high. Near the photosphere the finite-difference analog of rot**B** is rather different from zero for the initial potential field. So, the parasitic force $\mathbf{j} \times \mathbf{B}$ causes the numerical instability. Several methods have been used to stabilize the solution. The finite-difference scheme used in PERESVET code is absolutely implicit. It is solved by the method of iterations.

The PERESVET code includes the multilevel time steps dividing. The time steps strongly decrease in the places of high gradients. The main time step dividing is

fulfilled near the photospheric boundary.

6.2. *The initial-boundary conditions and methods of solution that were not used in the present work, but had already been developed and tested*

More precise calculations assume setting the initial potential field corresponding to initial distribution of the vertical magnetic component measured on the photosphere. The solution with such initial magnetic field must better describe the details of the processes in the solar corona. Also for such approximation of the potential magnetic field values in the points of corresponding numerical net, that finite-difference analog of div**B**, and rot**B** are equal to zero with very high precision, the solution becomes more stable, if the difference scheme conservative relative to magnetic flux is used. The method of setting of such initial potential field approximation is realized now in modernized code PERESVET, in which the conservative relative to magnetic flux scheme is used. It was tested for Bastille flare active region for photosphere field as approximated by set of dipoles as taken directly from observational date.

For stabilizing of solution the artificial viscosity is also used for smoothing a solution. The solution is stabilized near the boundary, but distributions are also smoothed in the CS, where values must be changed very steep. So, in the new version of PERESVET code the artificial viscosity can be set only near the photospheric boundary.

If the region of calculations is large, then the nonphotospheric boundary is located far from spots, and the magnetic field on this boundary is much smaller than above the spots. In this case there are no problems in setting the magnetic field on the non-photospheric boundary. But for the net $41\times41\times41$, which has been used, the space step becomes too large, and the processes near the sheet are simulated roughly. If the numerical region has a small size, then some nonphysical processes can be caused by the boundary conditions. To demonstrate this effect the simulations have been done for a large and a small regions. Comparison of these calculations permits to separate unphysical processes and helps to investigate detailed behavior of solutions in the vicinity of a CS.

All described methods help to get the stable solution using a personal computer on the $41\times41\times41$ net. It is possible that all these methods are not needed in simulation for such active region, if the supercomputer is used, and so, the size of the net is sufficiently large. But even for a supercomputer, if the active region is much more complicated, for example, if it contains more then 10 spots and several singular lines, then these methods are necessary.

The calculations show that the instability grows on the photospheric boundary during the long run, even if the artificial magnetic viscosity is used and the disturbances on the photosphere are small. It can be explained by such a way. The magnetic viscosity effectively stabilize solution only, if the viscosity term is represented as finite-difference analog of $\Delta\mathbf{B}$, because $\Delta\mathbf{B}$ contains the derivatives of the same components of **B** as in the left part of the equation $\partial\mathbf{B}/\partial t=\mathbf{rot}\,(\mathbf{V}\times\mathbf{B})+\nu_{\mathrm{m}}\Delta\mathbf{B}$. Here $\Delta\mathbf{B}=-\mathrm{rot}\,(\mathrm{rot}\mathbf{B})$, because of div**B**=0. Such presentation permits to avoid numerical solution (usually unstable) of the equation $\partial\mathbf{B}/\partial t=\mathbf{rot}\,(\mathbf{V}\times\mathbf{B})-\nu_{\mathrm{m}}\mathrm{rot}\,(\mathrm{rot}\mathbf{B})$, which contains derivatives of different components of **B**. But finite-difference analog of div**B** is

not exactly zero.   The error is proportional to the net space step.   So, at solving the equation $\partial \mathbf{B}/\partial t = \mathbf{rot}(\mathbf{V} \times \mathbf{B}) + \nu_m \Delta \mathbf{B}$ the current never relaxes to zero near the photospheric boundary (where gradient of B is high).   As a result, after long time calculations, even a small parasitic force $\mathbf{j} \times \mathbf{B}$ causes the instability.   To stabilize it the conservative relative to magnetic flux scheme is developed, in which finite-difference analog of div$\mathbf{B}$ equal to zero with high precision must be used.   In this scheme it is used the averaged magnetic fluxes through the boundaries of numerical cells instead of field vectors in the points of the grid.   This scheme is realized in the new version of PERESVET code and is already tested for photospheric magnetic field distributions of Bastille flare active region obtained as from approximation by dipoles as directly ffom observational data.

6.3.   The initial-boundary conditions and methods of solution that should be developed to solve present difficulties in future

There are several possibilities that can realize for setting of the nonpotential initial field by including appropriate procedures in the PERESVET code.   One of them consists in finding of a solution of stationary finite-difference scheme by relaxation in time of the solution of a nonstationary scheme.   Another method of setting the initial magnetic field consists in solving of the MHD equations for zero initial magnetic field, and changing the photospheric magnetic field from zero one to required distribution. Under rather high diffusion conditions the current must damp, and the magnetic field becomes the potential one.   Now these methods are introduced in PERESVET code, but it is not tested.

Also it is planned to modernize the numerical scheme such a way, that the space step is strongly decrease in the places of strong values gradient and it will be remained all other useful properties of the scheme (absolute implicit, conservative relative to magnetic flux and others).

7.   Conclusion

These investigations are directed for tracing the chain of phenomena that appear on the Sun and initiate solar flares and CMEs.   These two processes are associated: both of them are manifestations of the same explosive energy release.   Depending on conditions the explosive energy release can have one or other manifestation or both of them.   The energy for this explosive process is accumulated high in the corona in a current sheet above the active region.   The current sheet is created in the vicinity of a magnetic field singular line by focusing of disturbances, which come from the photosphere.   The MHD simulation of a current sheet in the corona, which uses the observed magnetic charts on the photosphere as boundary conditions, can improve the solar flare and CME prediction.   The CME appears due to the plasma acceleration along the current sheet by the magnetic tension forces.   One of the main parameters, which control CME (and such a way susubstorms occurrence) is the angle of the current sheet inclination to the photosphere.   The angle of current sheet inclination can be obtained from MHD simulation results.

Acknowledgments

The editor thanks Dr. K. Marubashi and another referee for their help in evaluating this paper.

References

Bilenko, I., Podgorny, A.I. and Podgorny, I.M. (2002): The possibility of energy accumulation in a current sheet above the NOAA 9077 active region prior to the flare on 14 July 2000. Solar Phys., **207**, 323–336.

Cox, D.P. and Tucker, W.H. (1969): Ionization equilibrium and radiative cooling of a low-density plasma. Astrophys. J., **157**, 1157–1167.

Demoulin, P., Henoux J.C. and Mandrini, C.H. (1992): Development of a topological model for solar flares. Solar Phys., **139**, 105–123.

Dryer, M. (1996): Comments on the origins of coronal mass ejections. Solar Phys., **169**, 421–429.

Hiei, E. and Hundhausen, A.J. (1996): Development of a coronal helmet streamer of 24 January 1992. Magnetospheric Phenomena in the Solar Atmosphere, ed. by Y. Uchida *et al.* Dordrecht, Kluwer Academic Publ., 125–126.

Podgorny, A.I. (1989): On the possibility of the solar flare energy accumulation in the vicinity of a singular line. Solar Phys., **123**, 285–308.

Podgorny, A.I. (1995): Numerical simulation of the current sheet above solar spots. Solar Phys., **156**, 41–64.

Podgorny, A.I. and Podgorny, I.M. (1992): A solar flare model including the formation and destruction of the current sheet in the corona. Solar Phys., **139**, 125–145.

Podgorny, A.I. and Podgorny, I.M. (1998): Numerical simulation of a current sheet during the flare of May, 30 1991. Solar Phys., **182**, 159–162.

Podgorny, A.I. and Podgorny, I.M. (1999): The associaton of flares and transients. Proceedings of 22nd Annual Seminar "Physics of Auroral Phenomena", Apatity, 73–76.

Podgorny, A.I. and Podgorny, I.M. (2001): Numerical simulation of solar flare produced by emergence of new magnetic flux. Astron. Rep., **45**, 60–66.

Podgorny, A.I., Podgorny, I.M. and Minami, S. (2000): Numerical simulation of current sheet creation above real active region. Adv. Space Res., **26**, 535–538.

Shibata, K. (1996): Dynamical processes in the solar corona. Magnetodynamic Phenomena in the Solar Atmosphere, ed. by Y. Uchida *et al.* Dordrecht, Kluwer Academic Publ., 13–20.

Zhang, J., Dere, K.P. and Howard, R.A. (2001): On the temporal relationship between coronal mass ejections and flares. Astrophys. J., **559**, 452–462.